Maximizing Energy Charging for UAV-assisted MEC Systems with SWIPT

Xiaoyan Hu, *Member, IEEE,* Pengle Wen, *Student Member, IEEE,*
Han Xiao, *Student Member, IEEE,* Wenjie Wang, *Member, IEEE,* Kai-Kit Wong, *Fellow, IEEE*

***Abstract*—A Unmanned aerial vehicle (UAV)-assisted mobile edge computing (MEC) scheme with simultaneous wireless information and power transfer (SWIPT) is proposed in this paper. Unlike existing MEC-WPT schemes that disregard the downlink period for returning computing results to the ground equipment (GEs), our proposed scheme actively considers and capitalizes on this period. By leveraging the SWIPT technique, the assistant UAV can simultaneously transmit energy and the computing results during the downlink period. In this scheme, our objective is to maximize the remaining energy among all GEs by jointly optimizing computing task scheduling, UAV transmit and receive beamforming, BS receive beamforming, GEs' transmit power and power splitting ratio for information decoding, time scheduling, and UAV trajectory. We propose an alternating optimization algorithm that utilizes the semidefinite relaxation (SDR), singular value decomposition (SVD), and fractional programming (FP) methods to effectively solve the non-convex problem. Numerous experiments validate the effectiveness of the proposed scheme.**

***Index Terms*— Mobile edge computing (MEC), simultaneous wireless information and power transfer (SWIPT), unmanned aerial vehicle (UAV).**

I. Introduction

The technology of mobile edge computing (MEC) enables users to offload computing tasks to the nearby edge servers for processing, which significantly reduces the computing latency and the energy consumption of the user devices. The practical applications and future development trends of MEC have been extensively studied in [1]. In general, edge computing servers are fixed on the ground in the traditional MEC systems, potentially resulting in limited service coverage. Integrating unmanned aerial vehicles (UAVs) with MEC can overcome these limitations, enhancing coverage and improving the efficiency of the MEC system due to their impressive mobility and flexibility. Specifically, in [2], the authors explored a MEC framework supported by a UAV, where the UAV can act as a computing server to assist ground equipment (GE) in processing computing tasks and serve as a relay to further offload GEs' computation tasks to the base station (BS).

While the MEC technology is capable of processing GEs' computation tasks remotely, it cannot work well in scenarios where the GEs' battery power is insufficient and may demand additional energy to sustain normal operations including task offloading. Hence, leveraging the technology of wireless charging into the MEC systems can help address this energy-insufficiency problem [3]–[6]. In [4], a UAV-enabled MEC system is explored, where the UAV initially charges the GEs using wireless power transfer (WPT), and then each GE sends its tasks to the UAV for processing. The maximization of the computation energy efficiency for a non-orthogonal multiple access (NOMA)-based WPT-MEC network is studied in [5]. Additionally, a UAV-MEC system with WPT from UAV to GEs as well as from BS to UAV is explored in [6].

Note that most existing MEC works assume that the sizes of the computation results are small, and thus the downlink period for returning these results to GEs is usually ignored. This assumption does not align with some practical applications with large volumes of computation results. For the applications such as high-resolution image processing, the UAV or the BS assists in processing the image data from GEs, and the sizes of the computing results may exceed those initial offloaded data [7]. To guarantee the accuracy, it is necessary to consider the downlink period for transmitting the task results from the UAV or BS to GEs in certain practical scenarios. Moreover, we can capitalize on the technology of the simultaneous wireless information and power transfer (SWIPT) to transmit energy and results data simultaneously while still meeting the computation latency requirements during this period, aiming at enhancing the efficiency and accuracy of the system.

Motivated by the above analysis, we explore a UAV-assisted MEC system considering both uplink and downlink periods. The contributions of this paper are summarized below.

- We investigate a practical scenario of UAV-assisted MEC network considering both uplink computation offloading and downlink results transmission. The SWIPT technology is leveraged for simultaneously downlink energy and data transmission, so as to improve system efficiency.
- An optimization problem is established aiming at maximizing the minimum remaining energy among all GEs, through jointly designing the computing task scheduling, transmit and receive beamforming of UAV, receive beamforming of BS, transmit and receive power splitting ratio of GEs, time scheduling, and UAV trajectory.
- To effectively solve the formulated non-convex optimiza-

This work is supported in part by the National Natural Science Foundation of China (NSFC) under Grant 62201449, in part by the Young Elite Scientists Sponsorship Program by CAST under Grant No.YESS20230611, in part by the Key R&D Projects of Shaanxi Province under Grant 2023-YBGY-040, in part by the Qin Chuang Yuan High-Level Innovation and Entrepreneurship Talent Program under Grant QCYRCXM-2022-231, and in part by the "Si Yuan Scholar" Foundation. *(Corresponding author: Xiaoyan Hu.)*

X. Hu, P. Wen, H. Xiao, and W. Wang, are with the School of Information and Communications Engineering, Xi'an Jiaotong University, Xi'an 710049, China. (email: xiaoyanhu@xjtu.edu.cn, pengle_wen@stu.xjtu.edu.cn, hanxiaonuli@stu.xjtu.edu.cn, wjwang@mail.xjtu.edu.cn).

K.-K. Wong is with the Department of Electronic and Electrical Engineering, University College London, London WC1E 7JE, U.K. (email: kai-kit.wong@ucl.ac.uk)

tion problem, we propose an alternating optimization algorithm based on semidefinite relaxation (SDR), singular value decomposition (SVD) and fractional programming (FP) techniques. With these methods, the closed-form expressions of uplink-period beamforming, the optimal resource allocation, the downlink-period beamforming solution and the UAV trajectory are respectively derived in four sub-problems with less complexity and higher accuracy. The simulation results indicate that the proposed UAV-assisted MEC-SWIPT scheme can significantly outperform the benchmark schemes.

II. System Model and Problem Formulation

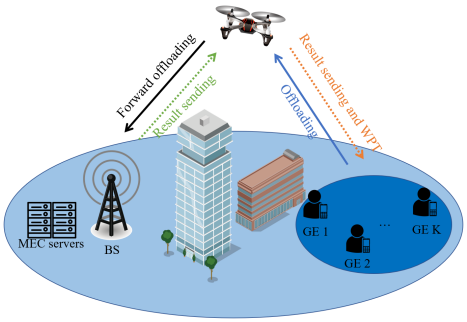

Fig. 1. The model of UAV-assisted MEC-SWIPT system.

As depicted in Fig. 1, we consider a UAV-assisted MEC-SWIPT network, which consists of a BS co-located with a MEC server, a UAV, and K GEs. Each GE $k \in \mathcal{K} \triangleq \{1, ..., K\}$ has a computation-intensive task that is bit-wise independent and requires extra electrical supply to maintain normal operations. We assume that the direct links between GEs and the BS are blocked by buildings. The assistant UAV, equipped with L antennas, acts as a relay to send GEs' offloaded tasks to the BS for processing during the uplink period. Additionally, the SWIPT technology is leveraged by the UAV to transmit the computation results back to the GEs and engage in wireless charging for GEs simultaneously during the downlink period. The BS is equipped with a uniform rectangular array of $M = M_{\mathrm{x}} M_{\mathrm{y}}$ antennas, respectively with M_{x} and M_{y} elements along each x-direction and y-direction.

The system is modeled in a three-dimensional (3D) Euclidean coordinate system for all nodes. We divide the flight time T into N time slots, each slot $n \in \mathcal{N} \triangleq \{1, \cdots, N\}$ with the length of $\delta = \frac{T}{N}$, where δ is sufficiently small such that the UAV's location can be assumed to be unchanged during each slot. The BS and GE $k \in \mathcal{K}$ are located horizontally at $\mathbf{s}_{\mathrm{b}} = (x_{\mathrm{b}}, y_{\mathrm{b}})$ and $\mathbf{s}_k = (x_k, y_k)$, with zero vertical coordinates. The UAV is assumed to fly at a fixed altitude $H > 0$ and its horizontal locations at the n-th time slot are denoted as $\mathbf{q}[n] = (x_{\mathrm{u}}[n], y_{\mathrm{u}}[n])$. The initial and final horizontal locations of the UAV are set as $\mathbf{q}_{\mathrm{I}} = (x_{\mathrm{I}}, y_{\mathrm{I}})$ and $\mathbf{q}_{\mathrm{F}} = (x_{\mathrm{F}}, y_{\mathrm{F}})$, respectively, and the maximum flight speed of the UAV is assumed to be $V_{\max}$. Hence, the UAV must satisfy the following mobility constraints

$$\|\mathbf{q}[n+1] - \mathbf{q}[n]\| \leq \delta V_{\max}, \ \forall n = 1, \cdots, N-1, \quad (1)$$

$$\mathbf{q}[1] = \mathbf{q}_{\mathrm{I}}, \ \mathbf{q}[N] = \mathbf{q}_{\mathrm{F}}. \quad (2)$$

A. Channel Model

Similar to [8], we adopt the Rician channel to model the GE-UAV links and the UAV-BS link. Therefore, we have

$$\mathbf{h}_z[n] = \sqrt{\frac{\beta_0}{d_z^2[n]}}\left(\sqrt{\frac{\zeta}{1+\zeta}}\mathbf{h}_z^{\mathrm{LoS}}[n] + \sqrt{\frac{1}{1+\zeta}}\mathbf{h}_z^{\mathrm{NLoS}}[n]\right), \quad (3)$$

where $z \in \{\{k, \mathrm{u}\}, \{\mathrm{u,b}\}\}$ indicates the subscripts of the GE k-UAV and the UAV-BS links, β_0 is the average channel power gain at a reference distance of 1 meter (m), ζ denotes the Rician factor. Besides, $d_{k,\mathrm{u}}[n] = \sqrt{\|\mathbf{q}[n] - \mathbf{s}_k\|^2 + H^2}$ and $d_{\mathrm{u,b}}[n] = \sqrt{\|\mathbf{q}[n] - \mathbf{s}_{\mathrm{b}}\|^2 + H^2}$ are the distances from GE k to the UAV and from the UAV to the BS, respectively.

For the Line of Sight (LoS) component, we have $\mathbf{h}_{k,\mathrm{u}}^{\mathrm{LoS}}[n] = \left[1, e^{-j\frac{2\pi}{\lambda}d\Phi_{k,\mathrm{u}}[n]}, \ldots, e^{-j\frac{2\pi}{\lambda}d(L-1)\Phi_{k,\mathrm{u}}[n]}\right]^T \in \mathbb{C}^{L\times 1}$, where λ represents the carrier wavelength, d is the uniform distance between antennas, and $\Phi_{k,\mathrm{u}}[n] = \frac{x_{\mathrm{u}}[n] - x_k}{d_{k,\mathrm{u}}[n]}$ indicates the cosine of the angle of arrival (AoA) for the signal from GE k to the UAV. In addition[1], $\mathbf{H}_{\mathrm{u,b}}^{\mathrm{LoS}}[n] = \boldsymbol{\phi}_{\mathrm{b,r}}[n]\boldsymbol{\phi}_{\mathrm{u,b}}^H[n] \in \mathbb{C}^{M_{\mathrm{x}}M_{\mathrm{y}}\times L}$, where $\boldsymbol{\phi}_{\mathrm{u,b}}[n] = \left[1, e^{-j\frac{2\pi}{\lambda}d\varphi_{\mathrm{ub}}[n]}, \ldots, e^{-j\frac{2\pi}{\lambda}d(L-1)\varphi_{\mathrm{ub}}[n]}\right]^T \in \mathbb{C}^{L\times 1}$ denotes the array response with respect to (w.r.t.) the angle of departure (AoD) for the signal from the UAV to the BS with $\varphi_{\mathrm{ub}}[n] = \frac{x_{\mathrm{b}} - x_{\mathrm{u}}[n]}{d_{\mathrm{u,b}}[n]}$ being the cosine of the AoD, and $\boldsymbol{\phi}_{\mathrm{b,r}}[n] = \left[1, e^{-j\frac{2\pi}{\lambda}d\varphi_{\mathrm{br,x}}[n]}, \ldots, e^{-j\frac{2\pi}{\lambda}d(M_{\mathrm{x}}-1)\varphi_{\mathrm{br,x}}[n]}\right]^T \otimes \left[1, e^{-j\frac{2\pi}{\lambda}d\varphi_{\mathrm{br,y}}[n]}, \ldots, e^{-j\frac{2\pi}{\lambda}d(M_{\mathrm{y}}-1)\varphi_{\mathrm{br,y}}[n]}\right]^T \in \mathbb{C}^{M_{\mathrm{x}}M_{\mathrm{y}}\times 1}$ indicates the receive array response at the BS, with $\varphi_{\mathrm{br,x}}[n] = \sin\varpi[n]\sin\Theta[n]$ and $\varphi_{\mathrm{br,y}}[n] = \sin\varpi[n]\cos\Theta[n]$ respectively denoting the vertical and horizontal AoAs of the signals from the UAV to the BS. Here we have $\sin\varpi[n] = \frac{H}{d_{\mathrm{u,b}}[n]}$, $\sin\Theta[n] = \frac{x_{\mathrm{b}} - x_{\mathrm{u}}[n]}{\sqrt{\|\mathbf{q}[n] - \mathbf{s}_{\mathrm{b}}\|^2}}$, and $\cos\Theta[n] = \frac{y_{\mathrm{b}} - y_{\mathrm{u}}[n]}{\sqrt{\|\mathbf{q}[n] - \mathbf{s}_{\mathrm{b}}\|^2}}$.

Without loss of generality, we assume that the Non-LoS (NLoS) components $\mathbf{h}_{k,\mathrm{u}}^{\mathrm{NLoS}}[n] \in \mathbb{C}^{L\times 1}$ and $\mathbf{H}_{\mathrm{u,b}}^{\mathrm{NLoS}}[n] \in \mathbb{C}^{M\times L}$ follow the complex normal distributions of $\mathcal{CN}(\mathbf{0}, \mathbf{I}_L)$ and $\mathcal{CN}(\mathbf{0}, \mathbf{I}_{M\times L})$, respectively. It is assumed that the channel reciprocity holds for all the uplink and downlink channels considered in this paper. For simplicity of expression, we define $\overline{\mathbf{H}}_{\mathrm{u,b}}[n] = \mathbf{H}_{\mathrm{u,b}}[n]\, d_{\mathrm{u,b}}[n]$ and $\overline{\mathbf{h}}_{k,\mathrm{u}}[n] = \mathbf{h}_{k,\mathrm{u}}[n]\, d_{k,\mathrm{u}}[n]$.

B. Computation and SWIPT Models

Base on the above analysis, the signal-to-interference-plus-noise ratio (SINR) of GE k's signal recovered at the UAV in time slot n for $k \in \mathcal{K}$ and $n \in \mathcal{N}$ can be expressed as

$$r_k[n] = \frac{\frac{E_k[n]}{t_{\mathrm{o}}[n]}\left|\mathbf{v}_k^H[n]\,\mathbf{h}_{k,\mathrm{u}}[n]\right|^2}{\sum_{j\neq k}^{K}\frac{E_j[n]}{t_{\mathrm{o}}[n]}\left|\mathbf{v}_k^H[n]\,\mathbf{h}_{j,\mathrm{u}}[n]\right|^2 + \|\mathbf{v}_k[n]\|^2\sigma^2}, \quad (4)$$

where $\mathbf{v}_k[n] \in \mathbb{C}^{L\times 1}$ represents the receive beamforming vector at the UAV for GE k, while $E_k[n]$ and $t_{\mathrm{o}}[n]$ respectively denote the transmit energy consumption of GE k and the allocated time for uplink offloading at time slot n. Additionally, σ^2 indicates the noise power at the receiver.

Furthermore, the transmission rate of the UAV for uplink task offloading to the BS at time slot n can be written as

$$R_{\mathrm{o,u}}[n] = B\log_2\det\left(\mathbf{I}_M + \Theta_{\mathrm{o,u}}[n]\right), \ \forall n, \quad (5)$$

[1]We use the capital letter $\mathbf{H}_{\mathrm{u,b}}$ to represent the UAV-BS channel considering the fact that it is a matrix instead of a vector.

where $\Theta_{\mathrm{o,u}}[n] = \mathbf{U}_{\mathrm{BS}}^H[n]\mathbf{H}_{\mathrm{u,b}}[n]\mathbf{U}_{\mathrm{UAV}}[n]\mathbf{U}_{\mathrm{UAV}}^H[n]\mathbf{H}_{\mathrm{u,b}}^H[n]\mathbf{U}_{\mathrm{BS}}[n]\left(\sigma^2\mathbf{U}_{\mathrm{BS}}^H[n]\mathbf{U}_{\mathrm{BS}}[n]\right)^{-1}$, with $\mathbf{U}_{\mathrm{UAV}}[n] \in \mathbb{C}^{L\times L}$ being the transmit covariance matrix of the UAV and $\mathbf{U}_{\mathrm{BS}}[n] \in \mathbb{C}^{M\times M}$ denoting the BS's receive covariance matrix. The allocated time for UAV's offloading is denoted as $t_u[n]$ in slot n.

Considering the downlink period for transmitting the computation results from the BS to GEs via the UAV, we assume that each GE applies the power splitting (PS) protocol to coordinate the processes of information decoding and energy harvesting from the received signal relayed by the UAV [9]. The received signal at GE k is split to the information decoder (ID) and the energy harvester (EH) by a power splitter. Define $\rho_k[n]$ as the portion of the signal power to the ID, while the remaining power is used by the EH. Therefore, the SINR and the harvested energy of GE k at time slot n are given by

$$r_{\mathrm{u},k}[n] = \frac{\rho_k\left[n\right]\left|\mathbf{h}_{k,\mathrm{u}}^H[n]\mathbf{w}_k\left[n\right]\right|^2}{\rho_k\left[n\right]\left(\sum_{j\neq k}^K\left|\mathbf{h}_{k,\mathrm{u}}^H[n]\mathbf{w}_j\left[n\right]\right|^2+\sigma_k^2\right)+\delta_k^2}, \tag{6}$$

$$E_k^{\mathrm{har}}[n] = t_{\mathrm{d}}\zeta_k\left(1-\rho_k\left[n\right]\right)\Big(\sum_{j=1}^K\left|\mathbf{h}_{k,\mathrm{u}}^H\left[n\right]\mathbf{w}_j\left[n\right]\right|^2+\sigma_k^2\Big), \tag{7}$$

where $\mathbf{w}_k\left[n\right] \in \mathbb{C}^{L\times 1}$ denotes the transmit beamforming of the UAV for GE k and $t_{\mathrm{d}} \in [0,\delta]$ indicates the predetermined time for the downloading period in each time slot. σ_k^2 is the noise power at GE k, while δ_k^2 represents the additional noise power introduced by the ID at GE k. Besides, $0 < \zeta_k \leq 1$ is the energy conversion efficiency at the EH of GE k.

Let $L_{\mathrm{c},k}\left[n\right]$ and $L_{\mathrm{o},k}\left[n\right]$ respectively represent the local computing and the offloaded task bits at time slot n. We assume that each GE has a required volume of computing task bits to be handled in each time slot, denoted as Γ. Thus, we have the following task requirement constraints:

$$L_{\mathrm{c},k}\left[n\right] + L_{\mathrm{o},k}\left[n\right] \geq \Gamma,\ \forall k, \forall n. \tag{8}$$

Denote the maximum CPU frequency of GE k as $F_k^{\max}$, then we have the following local computing resource constraints:

$$L_{\mathrm{c},k}[n] \leq \delta F_k^{\max}/C_k,\ \forall k, \forall n, \tag{9}$$

where C_k is the number of required CPU cycles for computing one task bit at GE k. Based on [2], the energy consumption of GE k for local computing can be expressed as

$$E_k^{\mathrm{comp}}[n] = L_{\mathrm{c},k}^3\left[n\right]C_k^3\varsigma_k/\delta^2,\ \forall k, \forall n, \tag{10}$$

where ς_k is the effective capacitance coefficient of GE k.

Let $L_{\mathrm{o,u}}\left[n\right]$ denote the task bits that the UAV further offloads to the BS for processing at time slot n. In this paper, we assume that the computing time at the BS and the transmission time from the BS to the UAV are negligible. Then we have the following causal constraints for the offloading process:

$$L_{\mathrm{o},k}[n] \leq t_{\mathrm{o}}[n]B\log_2\left(1+r_k\left[n\right]\right),\ \forall k, \forall n, \tag{11}$$

$$L_{\mathrm{o,u}}\left[n\right] \leq t_u[n]R_{\mathrm{o,u}}\left[n\right],\ \forall n, \tag{12}$$

$$\sum\nolimits_{k=1}^K L_{\mathrm{o},k}[n] \leq L_{\mathrm{o,u}}[n],\ \forall n, \tag{13}$$

$$\theta L_{\mathrm{o},k}[n] \leq t_{\mathrm{d}}B\log_2(1+r_{\mathrm{u},k}[n]),\ \forall k, \forall n, \tag{14}$$

where θ represents the uniform size ratio of the calculation results to the computation tasks.

C. Problem Formulation

We introduce an auxiliary variable η to denote the minimum remaining energy among all GEs as shown in constraint (15c). Hence, the problem for maximizing η can be formulated as

$$\textbf{(P1)}\ \max_{\mathbf{\Psi}}\ \eta \tag{15a}$$

$$\text{s.t.}\ \ (1),(2),(8),(9),(11)-(14), \tag{15b}$$

$$\eta \leq \sum_{n=1}^N E_k^{\mathrm{har}}[n] - E_k^{\mathrm{comp}}[n] - E_k[n],\ \forall k, \tag{15c}$$

$$t_{\mathrm{o}}[n] + t_{\mathrm{u}}[n] \leq \delta - t_{\mathrm{d}},\ \forall n, \tag{15d}$$

$$\mathrm{tr}(\mathbf{U}_{\mathrm{UAV}}\mathbf{U}_{\mathrm{UAV}}^H) \leq P_{\mathrm{UAV}}^{\max},\ \forall n, \tag{15e}$$

$$\sum\nolimits_{j=1}^K\left|\mathbf{w}_j^H\left[n\right]\mathbf{w}_j\left[n\right]\right|^2 \leq P_{\mathrm{UAV}}^{\max},\ \forall n, \tag{15f}$$

$$0 \leq E_k[n] \leq P_k^{\max}t_{\mathrm{o}}[n],\ \forall n, \forall k, \tag{15g}$$

$$0 \leq \rho_k\left[n\right] \leq 1,\ \forall k, \forall n. \tag{15h}$$

where constraints in (15d) ensure that the time allocated for uplink and downlink periods does not exceed the duration of each time slot. Additionally, (15e) and (15f) represent the power constraints of the UAV for uplink and downlink transmissions, while (15g) includes the offloading power constraints for GE k, where $P_{\mathrm{UAV}}^{\max}$ and $P_k^{\max}$ are the maximum transmit power of the UAV and the GE k, respectively. In addition, $\mathbf{\Psi} = \{\mathbf{v}_k\left[n\right], \mathbf{U}_{\mathrm{UAV}}\left[n\right], \mathbf{U}_{\mathrm{BS}}\left[n\right], \eta, t_{\mathrm{o}}\left[n\right], t_{\mathrm{u}}\left[n\right], E_k\left[n\right], L_{\mathrm{c},k}\left[n\right], L_{\mathrm{o},k}\left[n\right], \rho_k\left[n\right], \mathbf{w}_k\left[n\right], \mathbf{q}\left[n\right]\}_{k\in\mathcal{K},n\in\mathcal{N}}$ denotes the compact set of the optimization variables. It is easy to note that the formulated problem (P1) is non-convex because of the strong couplings among variables in constraints (11)-(14).

III. Algorithm Design and Analysis

In this section, we propose an alternating optimization algorithm to solve the problem (P1). We divide the optimization variables into four blocks, i.e., the uplink-period beamforming design set $\mathbf{\Psi}_1 = \{\mathbf{v}_k\left[n\right], \mathbf{U}_{\mathrm{UAV}}\left[n\right], \mathbf{U}_{\mathrm{BS}}\left[n\right]\}$, the resource allocation set $\mathbf{\Psi}_2 = \{\eta, t_{\mathrm{o}}[n], t_{\mathrm{u}}[n], E_k[n], L_{\mathrm{c},k}[n], L_{\mathrm{o},k}[n]\}$, the downlink-period beamforming and GEs' PS design set $\mathbf{\Psi}_3 = \{\eta, \rho_k[n], \mathbf{w}_k\left[n\right]\}$, and UAV trajectory design set $\mathbf{\Psi}_4 = \{\eta, \mathbf{q}[n]\}$. Therefore, we decompose (P1) into the following four subproblems, which are analyzed and solved as follows.

1) Subproblem for Optimizing the Uplink-Period Beamforming Design Set $\mathbf{\Psi}_1$: We employ the zero-forcing (ZF) technique to obtain $\mathbf{v}_k[n]$ and the Singular Value Decomposition (SVD)-based approach to analyze the transmission rate from the UAV to the BS. Based on [9], [10], we can derive the closed-form beamforming solutions as

$$\mathbf{v}_k[n] = \mathbf{\Upsilon}_k[n]\mathbf{\Upsilon}_k^H[n]\overline{\mathbf{h}}_{k,\mathrm{u}}[n]/\|\mathbf{\Upsilon}_k[n]\mathbf{\Upsilon}_k^H[n]\overline{\mathbf{h}}_{k,\mathrm{u}}\left[n\right]\|, \tag{16}$$

$$\mathbf{U}_{\mathrm{BS}}[n] = [\overline{\boldsymbol{\xi}}_1,\ldots,\overline{\boldsymbol{\xi}}_M],\ \mathbf{U}_{\mathrm{UAV}}[n] = [\widehat{\boldsymbol{\xi}}_1,\ldots,\widehat{\boldsymbol{\xi}}_L], \tag{17}$$

where $\mathbf{\Upsilon}_k[n]$ denotes the orthogonal basis for the null space of $\overline{\mathbf{H}}_{k,\mathrm{u}}^H[n] = [\overline{\mathbf{h}}_{1,\mathrm{u}}\left[n\right],...,\overline{\mathbf{h}}_{k-1,\mathrm{u}}\left[n\right],\overline{\mathbf{h}}_{k+1,\mathrm{u}}\left[n\right],...,\overline{\mathbf{h}}_{K,\mathrm{u}}\left[n\right]]^H$. In addition, $\overline{\boldsymbol{\xi}}_m \in \mathbb{R}^{M\times 1}$ and $\widehat{\boldsymbol{\xi}}_l \in \mathbb{R}^{L\times 1}$ are the normalized eigenvectors corresponding to the m-th and l-th eigenvalues of $\overline{\mathbf{H}}_{\mathrm{u,b}}\left[n\right]\overline{\mathbf{H}}_{\mathrm{u,b}}^H\left[n\right]$ and $\overline{\mathbf{H}}_{\mathrm{u,b}}^H\left[n\right]\overline{\mathbf{H}}_{\mathrm{u,b}}\left[n\right]$, respectively.

Hence, after applying the zero-forcing receive beamforming at the UAV, the offloading SINR for GE k in equation (4) can be further transformed as the following equation:

$$r_k[n] = \frac{\frac{E_k[n]}{t_o[n]} \left|\mathbf{v}_k^{\mathrm{H}}[n]\, \mathbf{h}_{k,\mathrm{u}}[n]\right|^2}{\sigma^2}, \tag{18}$$

where $\mathbf{v}_k[n]$ is given in (16) and we have $\|\mathbf{v}_k[\mathrm{n}]\|^2 = 1$.

Actually, the channel matrix $\overline{\mathbf{H}}_{\mathrm{u,b}}[n]$ can be divided into several parallel sub-channels through SVD. Then the transmission rate from the UAV to BS given in (5) can be equivalently re-formulated as follows

$$R_{\mathrm{o,u}}[n] = \sum_{i=1}^{\tau[n]} B\log_2\Big(1 + \frac{\lambda_i E^i_{\mathrm{UAV}}[n]}{t_{\mathrm{u}}[n] d^2_{\mathrm{u,b}}[n]\sigma^2}\Big), \tag{19}$$

where $\tau[n]$ represents the rank of $\overline{\mathbf{H}}_{\mathrm{u,b}}[n]$, and λ_i denotes the square of the i-th singular value of $\overline{\mathbf{H}}_{\mathrm{u,b}}[n]$. In addition, $E^i_{\mathrm{UAV}}[n]$ signifies the transmit energy assigned by the UAV to the i-th sub-channel at the n-th time slot. This SVD decoupling will significantly simplify the solving process of the following sub-problems and reduce the computational complexity.

2) Subproblem for Optimizing the Resource Allocation Set $\mathbf{\Psi}_2$: To facilitate the subsequent analysis, we introduce a new variable $L^i_{\mathrm{o,u}}[n]$, indicating the offloaded task bits from UAV to BS using the i-th sub-channel at time slot n. Additionally, we define a new optimization set for subproblem (P2), denoted as $\mathbf{\Psi}'_2 = \big\{\mathbf{\Psi}_2, \{L^i_{\mathrm{o,u}}[n], E^i_{\mathrm{UAV}}[n]\}_{\forall i,n}\big\}$. For any given variable sets $\mathbf{\Psi}_1$, $\mathbf{\Psi}_3$ and $\mathbf{\Psi}_4$, the corresponding subproblem (P2) for optimizing $\mathbf{\Psi}'_2$ can be expressed as

$$\textbf{(P2)} \quad \max_{\mathbf{\Psi}'_2} \quad \eta \tag{20a}$$

$$\text{s.t.} \quad (8), (9), (11), (13), (14), (15d), (15g), (15c), \tag{20b}$$

$$L_{\mathrm{o,u}}[n] \le \sum\nolimits_{i=1}^{\tau[n]} L^i_{\mathrm{o,u}}[n], \ \forall n, \tag{20c}$$

$$L^i_{\mathrm{o,u}}[n] \le t_{\mathrm{u}}[n] B\log_2\Big(1 + \frac{\lambda_i E^i_{\mathrm{UAV}}[n]}{t_{\mathrm{u}}[n] d^2_{\mathrm{u,b}}[n]\sigma^2}\Big), \ \forall n, \forall i, \tag{20d}$$

$$\sum\nolimits_{i=1}^{\tau[n]} E^i_{\mathrm{UAV}}[n] \le P^{\max}_{\mathrm{UAV}} t_{\mathrm{u}}[n], \ \forall n. \tag{20e}$$

Since $f(x,t) = t\log(1 + x/t)$ is a joint concave function w.r.t. x and t for case of $x, t \ge 0$ [11], then the constraints (11), (14), and (20d) are convex versus the variables in $\mathbf{\Psi}'_2$. Therefore, problem (P2) is a standard convex problem that can be effectively solved by the existing tools, such as CVX.

3) Subproblem for Optimizing the Downlink-Period Beamforming and GEs' PS Design Set $\mathbf{\Psi}_3$: By defining $\mathbf{W}_k[n] = \mathbf{w}_k[n]\mathbf{w}_k^H[n]$, $\mathbf{H}_{k,\mathrm{u}}[n] = \mathbf{h}_{k,\mathrm{u}}[n]\mathbf{h}^H_{k,\mathrm{u}}[n]$, and introducing an auxiliary variable $\widetilde{\rho}_k[n]$ that satisfys $e^{\widetilde{\rho}_k[n]} = \rho_k[n]$, then the constraints (14), (15c) and (15f) can be respectively re-expressed as follows:

$$\mathrm{tr}\left(\mathbf{H}_{k,\mathrm{u}}[n]\, \mathbf{W}_k[n]\right) \ge \Big(2^{\frac{\theta L_{\mathrm{o},k}[n]}{t_{\mathrm{d}} B}} - 1\Big) \times \Big(\sum\nolimits_{j\ne k}^{K} \mathrm{tr}\left(\mathbf{H}_{k,\mathrm{u}}[n]\, \mathbf{W}_j[n]\right) + \left(\delta_k^2 + \sigma^2\right) e^{-\widetilde{\rho}_k[n]}\Big), \ \forall n, \tag{21}$$

$$\sum_{n=1}^{N} t_{\mathrm{d}}\zeta_k\big(1 - e^{\widetilde{\rho}_k[n]}\big)\Big(\sum_{j=1}^{K} \mathrm{tr}\left(\mathbf{H}_{k,\mathrm{u}}[n]\, \mathbf{W}_j[n]\right) + \sigma_k^2\Big) - E_k^{\mathrm{total}}[n] \ge \eta, \ \forall k, \tag{22}$$

$$\sum\nolimits_{j=1}^{K} \mathrm{tr}\left(\mathbf{W}_j[n]\right) \le P^{\max}_{\mathrm{UAV}}, \ \forall n, \tag{23}$$

where $E_k^{\mathrm{total}}[n] = E_k^{\mathrm{comp}}[n] + E_k[n]$ denotes the total energy consumption of GE k for computing and offloading at time slot n. Furthermore, in order to deal with the coupling relationship between $e^{\widetilde{\rho}_k[n]}$ and $\sum_{j=1}^{K} \mathrm{tr}\left(\mathbf{H}_{k,\mathrm{u}}[n]\, \mathbf{W}_j[n]\right) + \sigma_k^2$, we introduce a slack variable $\Omega_k[n]$. Then the constraint (22) can be re-expressed as the form in (24)-(25):

$$\sum_{n=1}^{N} t_{\mathrm{d}}\zeta_k\big(e^{\Omega_k[n]} - e^{\widetilde{\rho}_k[n] + \Omega_k[n]}\big) - E_k^{\mathrm{total}}[n] \ge \eta, \ \forall k, \tag{24}$$

$$e^{\Omega_k[n]} \le \Big(\sum_{j=1}^{K} \mathrm{tr}\left(\mathbf{H}_{k,\mathrm{u}}[n]\, \mathbf{W}_j[n]\right) + \sigma_k^2\Big), \ \forall k, \forall n. \tag{25}$$

Hence, for any given variable sets $\mathbf{\Psi}_1$, $\mathbf{\Psi}'_2$ and $\mathbf{\Psi}_4$, the subproblem (P3) for optimizing $\mathbf{\Psi}_3$ can be expressed as

$$\textbf{(P3)} \quad \max_{\mathbf{\Psi}'_3 = \{\mathbf{W}_k[n], \widetilde{\rho}_k[n], \Omega_k[n]\}_{\forall k,n}, \eta} \quad \eta \tag{26a}$$

$$\text{s.t.} \quad (21), (23), (24), (25), \tag{26b}$$

$$0 \le e^{\widetilde{\rho}_k[n]} \le 1, \ \forall k, \forall n, \tag{26c}$$

$$\mathbf{W}_k[n] \succeq 0, \ \forall k, \forall n, \tag{26d}$$

$$\mathrm{Rank}(\mathbf{W}_k[n]) = 1, \ \forall k, \forall n, \tag{26e}$$

which is still a non-convex optimization because of the constraints (24) and (26e). Fortunately, $e^{\Omega_k[n]}$ in (24) is a convex function w.r.t $\Omega_k[n]$, and thus we can obtain its lower bound via its first-order Taylor expansion, which is given by

$$\xi_1\left(\Omega_k[n]\right) = e^{\Omega_k^{(\mathrm{m})}[n]} + e^{\Omega_k^{(\mathrm{m})}[n]}\big(\Omega_k[n] - \Omega_k^{(\mathrm{m})}[n]\big), \tag{27}$$

where $\Omega_k^{(\mathrm{m})}[n]$ is the obtained solution at the m-th iteration.

By using $\xi_1\left(\Omega_k[n]\right)$ in (24) and dropping the rank-1 constraint (26e), the SDR form of problem (P3) is given as

$$\textbf{(P3.1)} \quad \max_{\mathbf{\Psi}'_3 = \{\mathbf{W}_k[n], \widetilde{\rho}_k[n], \Omega_k[n]\}_{\forall k,n}, \eta} \quad \eta \tag{28a}$$

$$\text{s.t.} \quad (21), (23), (25), (26c), (26d), \tag{28b}$$

$$\sum_{n=1}^{N} t_{\mathrm{d}}\zeta_k\big(\xi_1\left(\Omega_k[n]\right) - e^{\widetilde{\rho}_k[n] + \Omega_k[n]}\big) - E_k^{\mathrm{total}}[n] \ge \eta, \forall k. \tag{28c}$$

It can be verified that problem (P3.1) is a standard convex problem that can be solved by CVX. Additionally, $\rho_k[n]$ can be obtained according to $e^{\widetilde{\rho}_k[n]} = \rho_k[n]$. However, the solution to (P3.1) may conflict with the rank-1 constraint (26e) in problem (P3). Fortunately, we can provide a method to directly construct the solution satisfying the rank-1 constraints based on the solution of (P3.1) in the following Theorem 1.

Theorem 1. *Suppose that the optimal feasible solution of problem (P3.1) are $\mathbf{W}_k^*[n]$,$\widetilde{\rho}_k^*[n]$ and $\Omega_k^*[n]$. There exists $\mathbf{W}_k^\star[n]$ satisfying $Rank(\mathbf{W}_k^\star[n]) = 1$ while the other variables $\widetilde{\rho}_k^*[n]$ and $\Omega_k^*[n]$ are still feasible solutions to the problem (P3.1). The corresponding $\mathbf{W}_k^*[n]$ is given by*

$$\mathbf{W}_k^\star[n] = \frac{\mathbf{W}_k^*[n]\, \mathbf{h}_{k,u}[n]\, \mathbf{h}^H_{k,u}[n]\, \mathbf{W}_k^*[n]}{\mathbf{h}^H_{k,u}[n]\, \mathbf{W}_k^*[n]\, \mathbf{h}_{k,u}[n]}. \tag{29}$$

Proof: According to (29), $\mathbf{h}^H_{k,\mathrm{u}}[n]\, \mathbf{W}_k^\star[n]\, \mathbf{h}_{k,\mathrm{u}}[n] = \mathbf{h}^H_{k,\mathrm{u}}[n]\, \mathbf{W}_k^*[n]\, \mathbf{h}_{k,\mathrm{u}}[n]$, and $\mathrm{tr}(\mathbf{W}_k^\star[n]) = \mathrm{tr}(\mathbf{W}_k^*[n])$ always hold, which indicates that $\mathbf{W}_k^\star[n]$, $\rho_k^*[n]$, and $\Omega_k^*[n]$ are still optimal solutions to (P3.1). The proof has been completed. ■

4) Subproblem for Optimizing the UAV Trajectory Design Set $\mathbf{\Psi}_4$: For any given variable sets $\mathbf{\Psi}_1$, $\mathbf{\Psi}_2'$ and $\mathbf{\Psi}_3'$, the subproblem to solve $\mathbf{\Psi}_4$ can be expressed as follows:

$$\textbf{(P4)} \max_{\mathbf{\Psi}_4} \quad \eta \tag{30a}$$

$$\text{s.t.} \sum_{n=1}^{N} t_{\mathrm{d}}(1-\rho_k[n])\zeta_k\left(\sum_{j=1}^{K}\frac{|\overline{\mathbf{h}}_{k,\mathrm{u}}^H[n]\mathbf{w}_j[n]|^2}{d_{k,\mathrm{u}}^2[n]}+\sigma_k^2\right) - E_k^{\mathrm{total}}[n] \geq \eta,\ \forall k, \tag{30b}$$

$$d_{k,\mathrm{u}}^2[n] \leq \frac{E_k[n]\left|\mathbf{v}_k^H[n]\overline{\mathbf{h}}_{k,\mathrm{u}}[n]\right|^2}{t_{\mathrm{o}}[n]\sigma_k^2\left(2^{\frac{L_{\mathrm{o},k}[n]}{t_{\mathrm{o}}[n]B}}-1\right)},\ \forall k,\forall n, \tag{30c}$$

$$d_{k,\mathrm{u}}^2[n] \leq \frac{-\rho_k[n]|\overline{\mathbf{h}}_{k,\mathrm{u}}^H[n]\mathbf{w}_k[n]|^2}{\left(\rho_k[n]\sigma_k^2+\delta_k^2\right)} + \frac{\rho_k[n]|\overline{\mathbf{h}}_{k,\mathrm{u}}^H[n]\mathbf{w}_k[n]|^2}{\left(2^{\frac{\theta L_{\mathrm{o},k}[n]}{t_{\mathrm{d}}B}}-1\right)\left(\rho_k[n]\sigma_k^2+\delta_k^2\right)},\ \forall k,\forall n, \tag{30d}$$

$$d_{\mathrm{u,b}}^2[n] \leq E_i^{\mathrm{UAV}}[n]\lambda_i/\sigma^2 t_{\mathrm{u}}[n]\left(2^{\frac{L_{\mathrm{o},\mathrm{u}}^i[n]}{t_{\mathrm{u}}[n]B}}-1\right),\ \forall n,\forall i. \tag{30e}$$

Note that the non-convexity of problem (P4) comes from the fractional constraint (30b). We further employ the fractional programming (FP) theory [12] to solve it, through which the constraint (30b) can be transformed into the following form:

$$\sum_{n=1}^{N} t_{\mathrm{d}}(1-\rho_k[n])\zeta_k\left(\sum_{j=1}^{K}|\overline{\mathbf{h}}_{k,\mathrm{u}}^H[n]\mathbf{w}_j[n]|^2\Lambda_k[n]+\sigma_k^2\right) - E_k^{\mathrm{total}}[n] \leq \eta,\ \forall k, \tag{31}$$

where $\Lambda_k[n] = 2y_k[n] - y_k^2[n]d_{\mathrm{u},k}^2[n]$ with $y_k[n]$ being an auxiliary variable. Given the trajectory of the UAV at the m-th iteration, i.e., $\mathbf{q}^{(m)}[n]$, the optimal $y_k[n]$ can be updated by

$$y_k[n] = \frac{1}{\|\mathbf{q}^{(m)}[n]-\mathbf{s}_k\|^2+H^2}. \tag{32}$$

It can be noted that problem (P4) with the constraint (31) is a convex optimization problem. Therefore, this form of problem (P4) can be solved by utilizing the solvers like CVX. The complete iterative optimization algorithm with FP method to solve sub-problem (P4) is outlined in Algorithm 1.

Algorithm 1: Algorithm for Sub-Problem (P4)

1: For given variable sets $\mathbf{\Psi}_1$, $\mathbf{\Psi}_2$, $\mathbf{\Psi}_3$, initialize $\mathbf{q}^{(0)}[n]$ into feasible values; set $\iota = 0$.
2: **repeat**
3: Given $\mathbf{q}^{(\iota)}$, update $y_k[n]$ by (32).
4: Update $\mathbf{q}^{(\iota+1)}[n]$ by solving problem (P4) with (31).
5: Set $\iota = \iota + 1$.
6: **Until**: the algorithm converges; output $\mathbf{q}^{(\iota)}[n]$.

5) Proposed Iterative Optimization Algorithm and Analysis: Based on the above analysis, we summarize the proposed iterative algorithm for solving initial problem (P1) in Algorithm 2. Note that the convergence of the proposed algorithm can be guaranteed, since we can always find a solution not worse than that of the previous iteration through this algorithm.

Algorithm 2: Algorithm for Initial Problem (P1)

1: Initialize $\mathbf{\Psi}_1^{(0)}$, $\mathbf{\Psi}_2^{(0)}$ $\mathbf{\Psi}_3^{(0)}$ and $\mathbf{\Psi}_4^{(0)}$ as feasible solution; set $m = 0$.
2: **repeat**
3: Given $\left(\mathbf{\Psi}_2^{(m)}, \mathbf{\Psi}_3^{(m)}, \mathbf{\Psi}_4^{(m)}\right)$, obtain $\mathbf{\Psi}_1^{(m+1)}$ according to (16) and (17) respectively.
4: Given $\left(\mathbf{\Psi}_1^{(m+1)}, \mathbf{\Psi}_3^{(m)}, \mathbf{\Psi}_4^{(m)}\right)$, obtain $\mathbf{\Psi}_2^{'(m+1)}$ by solving problem (P2) with CVX.
5: Given $\left(\mathbf{\Psi}_1^{(m+1)}, \mathbf{\Psi}_2^{'(m+1)}, \mathbf{\Psi}_4^{(m)}\right)$, obtain $\mathbf{\Psi}_3^{'(m+1)}$ by solving problem (P3.1) with SDR method and construct a solution satisfying constraint (26e) in Theorem 1.
6: Given $\left(\mathbf{\Psi}_1^{(m+1)}, \mathbf{\Psi}_2^{'(m+1)}, \mathbf{\Psi}_3^{'(m+1)}\right)$, obtain $\mathbf{\Psi}_4^{(m+1)}$ by using Algorithm 1.
7: Set $m = m + 1$.
8: **Until**: the algorithm converges; output $\mathbf{\Psi}$.

The computational complexity of the proposed Algorithm 2 primarily arises from Step 4 to Step 6 for solving problems (P2) to (P4). Note that there are a total of $O_2 = (1 + 2N + 3KN + 2\Sigma_{n=1}^{N}\tau[n])$ variables in $\mathbf{\Psi}_2'$, and thus the computational complexity of Step 4 for solving the convex problem (P2) with the interior point method in CVX is $\mathcal{O}_2 = \mathcal{O}(O_2^{3.5})$. Similarly, problems (P3.1) and (P4) have $O_3 = (1 + NK + KNL^2)$ and $O_4 = (1 + 2N)$ variables, then the computational complexity of Step 5 and Step 6 are respectively $\mathcal{O}_3 = \mathcal{O}(I_3(O_3^{3.5}))$ and $\mathcal{O}_4 = \mathcal{O}(I_4(O_4^{3.5}))$, where I_3 and I_4 are the corresponding number of iterations. In summary, the computational complexity of Algorithm 2 for solving the initial problem (P1) is $\mathcal{O}_{total} = (I(\mathcal{O}_2+\mathcal{O}_3+\mathcal{O}_4))$, where I denotes the number of outer iterations.

IV. Simulation Results

In this section, we simulate the case of K= 4 GEs with the coordinates of $(-10, -12)$, $(-5, -9)$, (5, -14), (13, -12) respectively. Besides, the other simulation parameters are set as $C_k = 1000$, β_0 = -20 dB, σ_k^2= -60 dBm, σ^2 = -60 dBm, δ_k^2 = -50 dBm, B = 10 MHz, ζ = 10 dB, ς_k = 10^{-28}, θ = 10^{-5}, $F_k^{\max}$ = 2 GHz, $P_k^{\max}$ = 1 W, M_{x} = 4, M_{y} = 4, δ = 0.5s, T= 10s, t_{d} = 0.5δ, ζ_k = 0.8, $\mathbf{q}_{\mathrm{I}}$= (-10, -14), $\mathbf{q}_{\mathrm{F}}$= (15, -7), $\mathbf{s}_{\mathrm{b}}$ = (3, -5) and $V_{\max}$ = 5m/s.

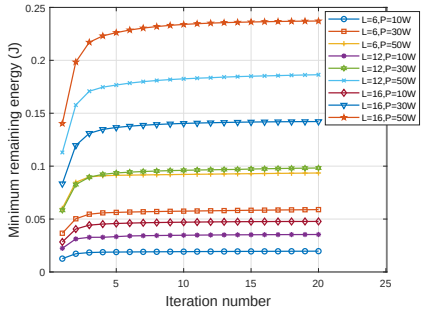

Fig. 2. The convergence performance of the proposed algorithm.

The curves in Fig. 2 illustrate the convergence performance of the proposed algorithm across different numbers of UAV

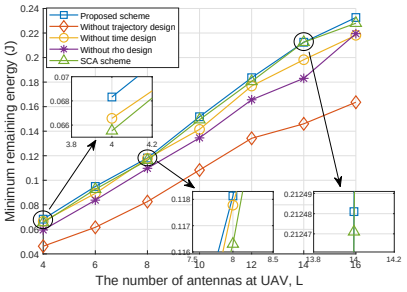

Fig. 3. Remaining energy versus the number of antennas at UAV with $P_{\mathrm{UAV}}^{\max}$ = 50W, H = 5m and Γ = 1Mb.

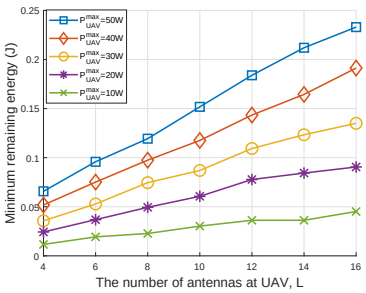

Fig. 4. Remaining energy versus transmit power with H = 5m and Γ = 1Mb.

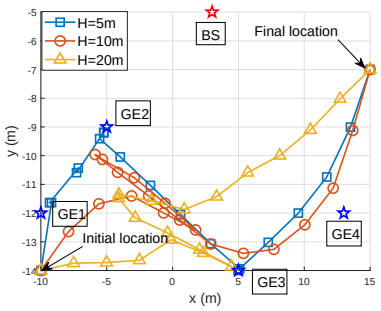

Fig. 5. UAV trajectory versus the UAV altitude with Γ = 1Mb, L = 8 and $P_{\mathrm{UAV}}^{\max}$ = 50W.

antennas and levels of transmit power. It is evident that, regardless of these variations, the values of minimum remaining energy initially increase and then gradually converge as the iteration increases, which can clearly verify the convergence of the proposed algorithm. In addition, the performance of the proposed scheme can be highly improved with larger number of UAV antennas or transmit power.

In Fig. 3, the performances of different schemes versus the varying numbers of UAV antennas are presented. The scheme without trajectory design refers to fixing the UAV's trajectory as the initial trajectory, while the scheme without time design refers to setting t_{o} and t_{u} as 0.25δ. The scheme without rho design refers to setting ρ_k as 0.1 for $k \in \mathcal{K}$, while the SCA scheme refers to optimizing the trajectory using the Successive Convex Approximation (SCA) method, representing a lower bound of the original problem. The performance of all schemes improves as the number of UAV antennas increases, as more antennas provide greater flexibility for beamforming. The proposed scheme is always superior to the other benchmark schemes, demonstrating its effectiveness in performance enhancement. The scheme without trajectory design exhibits inferior performance compared to our proposed scheme, suggesting that the UAV trajectory design can significantly improve the overall system performance. Furthermore, the scheme without rho design also exhibits a significant performance loss in comparison with the proposed scheme, which highlights the critical importance of designing the value of $\{\rho_k\}$ based on the requirements of the SWIPT networks.

We present the effects of transmit power on performance in Fig. 4 w.r.t. the number of UAV antennas. At low power levels, the system performance does not significantly improve with the increasing of antennas. However, as the power level increases, the system performance improves more significantly with the increasing number of UAV antennas. Especially when the power is 50W, the performance of the 16-antenna system improves by 254% compared to the 4-antenna system.

In Fig. 5, we compare the UAV trajectory at different altitudes. At an altitude of 5m, the UAV travels to each GE in sequence before flying to the final location. However, at altitudes of 10m or 20m, the UAV's trajectory tends to follow a more central route among GEs. As the altitude increases, the relative difference of distances between the UAV and GEs become smaller, making the more central trajectory more conducive to system performance.

V. Conclusions

In this paper, we propose a UAV-assisted MEC-SWIPT scheme, which enables the UAV to simultaneously transmit energy and computing results to GEs through the SWIPT technology. Then, we design an alternating optimization algorithm to maximize the minimum remaining energy among all GEs. The effectiveness of the proposed scheme is validated by comparing it with the baseline schemes. Simulation results show that the system performance can be significantly enhanced by designing UAV trajectories and GEs' PS ratio for information decoding. Additionally, the effect of the number of UAV antennas on system performance is also being examined.

References

[1] Y. C. Hu, M. Patel, D. Sabella, N. Sprecher, and V. Young, "Mobile edge computinga key technology towards 5g," *ETSI white paper*, vol. 11, no. 11, pp. 1–16, 2015.

[2] X. Hu, K.-K. Wong, K. Yang, and Z. Zheng, "UAV-assisted relaying and edge computing: Scheduling and trajectory optimization," *IEEE Transactions on Wireless Communications*, vol. 18, no. 10, pp. 4738–4752, 2019.

[3] X. Hu, K.-K. Wong, and K. Yang, "Wireless powered cooperation-assisted mobile edge computing," *IEEE Transactions on Wireless Communications*, vol. 17, no. 4, pp. 2375–2388, 2018.

[4] Y. Du, K. Yang, K. Wang, G. Zhang, Y. Zhao, and D. Chen, "Joint resources and workflow scheduling in UAV-enabled wirelessly-powered mec for iot systems," *IEEE Transactions on Vehicular Technology*, vol. 68, no. 10, pp. 10 187–10 200, 2019.

[5] L. Shi, Y. Ye, X. Chu, and G. Lu, "Computation energy efficiency maximization for a NOMA-based WPT-MEC network," *IEEE Internet of Things Journal*, vol. 8, no. 13, pp. 10 731–10 744, 2021.

[6] X. Hu, K.-K. Wong, and Y. Zhang, "Wireless-powered edge computing with cooperative UAV: Task, time scheduling and trajectory design," *IEEE Wireless Commun.*, vol. 19, no. 12, pp. 8083–8098, 2020.

[7] C. Ledig, L. Theis, F. Huszár, J. Caballero, A. Cunningham, A. Acosta, A. Aitken, A. Tejani, J. Totz, Z. Wang *et al.*, "Photo-realistic single image super-resolution using a generative adversarial network," in *Proceedings of the IEEE conference on computer vision and pattern recognition*, 2017, pp. 4681–4690.

[8] Y. Xu, T. Zhang, Y. Liu, D. Yang, L. Xiao, and M. Tao, "Computation capacity enhancement by joint UAV and RIS design in IoT," *IEEE Internet of Things Journal*, vol. 9, no. 20, pp. 20 590–20 603, 2022.

[9] Q. Shi, L. Liu, W. Xu, and R. Zhang, "Joint transmit beamforming and receive power splitting for MISO SWIPT systems," *IEEE Transactions on Wireless Communications*, vol. 13, no. 6, pp. 3269–3280, 2014.

[10] A. Goldsmith, *Wireless communications*. Cambridge university press, 2005.

[11] S. P. Boyd and L. Vandenberghe, *Convex optimization*. Cambridge university press, 2004.

[12] K. Shen and W. Yu, "Fractional programming for communication systemspart I: Power control and beamforming," *IEEE Transactions on Signal Processing*, vol. 66, no. 10, pp. 2616–2630, 2018.